Positron Emission Tomography in Aging and Dementia: Effect of Cerebral Atrophy

John B. Chawluk, Abass Alavi, Robert Dann, Howard I. Hurtig, Sanjiv Bais, Michael J. Kushner, Robert A. Zimmerman, and Martin Reivich

Department of Neurology, Cerebrovascular Research Center, and Department of Radiology, Hospital of the University of Pennsylvania, Philadelphia, Pennsylvania

The spatial resolution of current positron emission tomography (PET) scanners does not allow a distinction between cerebrospinal fluid (CSF) containing spaces and contiguous brain tissue. Data analysis strategies which therefore purport to quantify cerebral metabolism per unit mass brain tissue are in fact measuring a value which may be artifactually reduced due to contamination by CSF. We studied cerebral glucose metabolism (CMRglc) in 17 healthy elderly individuals and 24 patients with Alzheimer's dementia using [^{18}F]fluorodeoxyglucose and PET. All subjects underwent x-ray computed tomography (XCT) scanning at the time of their PET study. The XCT scans were analyzed volumetrically, in order to determine relative areas for ventricles, sulci, and brain tissue. Global CMRglc was calculated before and after correction for contamination by CSF (cerebral atrophy). A greater increase in global CMRglc after atrophy correction was seen in demented individuals compared with elderly controls (16.9% versus 9.0%, p < 0.0005). Additional preliminary data suggest that volumetric analysis of proton-NMR images may prove superior to analysis of XCT data in quantifying the degree of atrophy. Appropriate corrections for atrophy should be employed if current PET scanners are to accurately measure actual brain tissue metabolism in various pathologic states.

The pioneering nitrous oxide technique of Kety and Schmidt first enabled investigators to measure global cerebral blood flow and metabolism in living humans (*1*). Attention soon turned to applications of their method in various normal and pathologic states, including aging and senile dementia. Early reports of markedly reduced cerebral blood flow and oxygen consumption in demented patients (*2*) represented important initial findings, but did little to elucidate the pathophysiologic mechanisms underlying specific features of dementing illnesses. It was hoped that regional measurements of circulation and metabolism might provide greater insights into abnormalities characteristic of specific forms of dementia. Methods developed for quantifying isotope clearance of krypton-85 and xenon-133 permitted such a determination of regional patterns of cerebral blood flow (*3,4*). These techniques have suffered from poor spatial resolution, however, and an inability to measure glucose or oxygen metabolism directly.

Positron emission tomography (PET) scanning offers a clearcut advantage over isotope clearance techniques, in that quantitative data can be obtained on blood flow, metabolism, and other aspects of cerebral physiology. Moreover, these parameters can be measured in three dimensions, allowing heretofore unprecedented resolution in regional studies of human physiology. Nevertheless, the spatial resolution of PET scanners in current clinical use (10–20 mm in-slice) still does not allow delineation of sulcal patterns or ventricular margins. Therefore, atrophic changes may be averaged into regional or global calculations of metabolic rates determined by PET, and lead to significant errors in estimates of parenchymal metabolic rates per se. These errors would be of particular importance in PET studies of aging and dementia, where cerebral atrophy is especially prominent.

The introduction of volumetric methods for calculating ventricular and sulcal sizes from x-ray computed tomographic (XCT) data (*5,6*) has not only led to an increased ability to distinguish demented patients from

age-matched controls (6–8), but also offers a method for correcting errors in regional and global PET data which arise due to the comparatively limited spatial resolution of PET. We have applied a modification of these methods to calculate the degree of atrophy in patients with Alzheimer's disease and elderly controls, and have utilized this atrophy value to correct measurements of global rates of cerebral glucose metabolism by PET. Our findings demonstrate the significant effect of cerebral atrophy in PET studies of dementia and aging. Preliminary atrophy measurements from proton-nuclear magnetic resonance (NMR) images also address the question of which imaging modality (XCT or NMR) most accurately reflects atrophic brain changes.

PATIENTS AND METHODS

Twenty-four patients with the clinical diagnosis of Alzheimer's disease (Dementia of the Alzheimer's type, or DAT) and 17 elderly normal controls were studied using PET to measure cerebral glucose metabolism (CMRglc), and XCT scans to determine anatomic features. All patients and controls were evaluated by a neurologist, and underwent an extensive battery of psychometric tests. The diagnosis of Alzheimer's disease (DAT) was based upon DSM III criteria and criteria set forth by the NINCDS-ADRDA Work Group on Alzheimer's disease (9,10). Of the 24 DAT patients, 19 fulfilled the criteria for probable DAT, clinically defined as a progressive worsening of memory and other cognitive functions without a disturbance of consciousness, onset between ages 40 and 90 yr, in the absence of systemic disorders or other brain diseases that themselves could account for a progressive cognitive disorder. Five patients met criteria for possible DAT (10), in that a single gradually progressive cognitive deficit was present in the absence of other identifiable cause. All subjects scored 2 or less on Rosen's modification of the Hachinski Ischemia Scale (11), supporting the diagnosis of primary degenerative (nonischemic) dementia. The severity of dementia was assessed using the 30-point Mini-Mental State Examination (MMSE) of Folstein et al. (12). By this measure 11 patients had mild dementia (MMSE scores >20), six moderate dementia (MMSE scores 10–20), and seven severe DAT (MMSE scores <10). A subgroup of five demented patients (four mild, one severe) also underwent proton-NMR imaging. Demographic data on this patient population is presented in Table 1.

All subjects had measurements of CMRglc made using fluorine-18 fluorodeoxyglucose (FDG) and PET (13). The administration of isotope (0.1 mCi/kg) and blood sampling methods have been previously described (14). Subjects were fasted overnight before the PET studies, and multiple determinations of plasma glucose levels varied on the average only 4% (range 1–9%) for any single subject during the uptake and scanning periods. During uptake of isotope the subject lies supine with eyes open in a dimly lit room. The ears are unplugged to background ambient noise, which is kept to a minimum. Images of FDG activity are obtained using a PETT V tomogaph (15). This system has an effective in-plane resolution of 16.5 mm (FWHM), and simultaneously generates

TABLE 1
Study Group

Diagnosis	No. of subjects	Age range* (yr)	Mean age (yr) (s.d.)
Elderly controls	17	46–76	61 (9)
Alzheimer's disease (DAT)	24	53–80	65 (9)

* Age differences not statistically significant (Student t-test).

seven cross-sectional images of brain, 17.4 mm thick, along the rostrocaudal axis. Subjects are positioned with the head extended so that the orbitomeatal line is 20° from the vertical (−20°) and two 10–20 min scans yielding 14 image slices per session are performed. A minimum of 1 million counts per slice are collected. Between the first and second scans the subject is displaced relative to the scanner along the rostrocaudal axis so that the seven images from each scan (14 slices total) are intercalated by one-half a slice thickness. Metabolic rates are calculated using the operational equation of Sokoloff et al. (16). We use a lumped constant value of 0.522 and average rate constants, determined in our laboratory from nine young normal subjects (17). A metabolic rate for the whole brain (WB) has been operationally defined by averaging global metabolism using eight slices extending from the lowest slice containing occipital cortex rostrally up to and including the first slice containing the cingulate gyrus in continuity. Each image is displayed in four gray scales, and the area of the brain is defined by an ellipse fit to the 50% intensity cutoff. The total number of head counts within a larger ellipse circumscribing the field of view are used for the WB calculation; an effective volumetric "count density" is determined by dividing the total counts by the volume of the whole-brain region of interest (ROI). In determining this "uncorrected" WB metabolic rate no implicit corrections are made for ventricular or sulcal volumes.

All subjects also underwent XCT transaxial scanning at the time of their PET study. XCT scans were done on a GE 8800 scanner, with a spatial resolution of 0.64 mm × 0.64 mm, and 5-mm slice thickness. Proton-NMR scans (on the five subjects mentioned above) were performed with a GE 0.12 Tesla unit (1 mm × 1 mm in-slice resolution, 12 mm slice thickness). T₁-weighted images were obtained using saturation recovery pulse sequences and rapid pulse repetition rates (0.15 sec) (18). All anatomic scans were obtained in planes angled at −20°, the same angle as in our PET studies.

Proton-NMR and XCT sections extending from the lowest slice containing occipital cortex rostrally to the first slice containing cingulum in continuity were analyzed volumetrically using a method similar to that reported by Gado et al. (6). These levels correspond to those PET sections used for the WB metabolic rate calculations. To assure that the WB volumes analyzed for the atrophy determination by XCT or NMR, and those used in the PET measurement of WB glucose metabolism were similar, absolute WB volumes were calculated from the pixel size, slice thickness, and scanner scaling factors. In four subjects whose NMR and PET scans were compared in this fashion, the WB volume ratio was 0.99 (s.d. = 0.08) Dann R: unpublished data). It is therefore unlikely

that WB volume discrepancies would introduce any systematic errors in the atrophy correction.
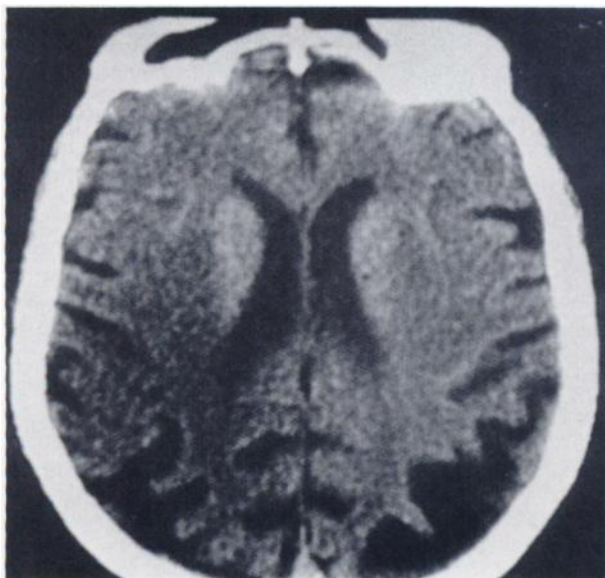
In order to quantify the degree of atrophy all anatomic images (XCT or NMR) were digitized using a Vidicon camera (DAGE) interfaced to a 6-bit digitizer. The images were displayed on a high resolution color monitor (Conrac) utilizing an image analysis system (Grinnell Systems) (Fig. 1). With these elements the resolution of digitization of the projected image is at least three times greater than that of the intrinsic XCT resolution. Areas of interest were then highlighted subjectively by way of a data tablet interface (Figs. 2–4), using nonoverlapping contiguous slices. The highlighted areas of interest on each slice correspond to the entire intracranial cavity (Fig. 2), the ventricular cavity (Fig. 3), and the sulcal plus cisternal spaces (Fig. 4). The number of pixels designated as ventricle or sulci on each slice is expressed as a percentage of the total number of pixels in that slice's intracranial cavity of interest, and these values are summated over all levels to obtain relative volumetric estimates of ventricular size, sulcal size, and "relative brain volume" (intracranial cavity minus [ventricle plus sulci]).

WB metabolic rates are then corrected for the degree of atrophy, assuming CSF to be metabolically inert, using the following formula:
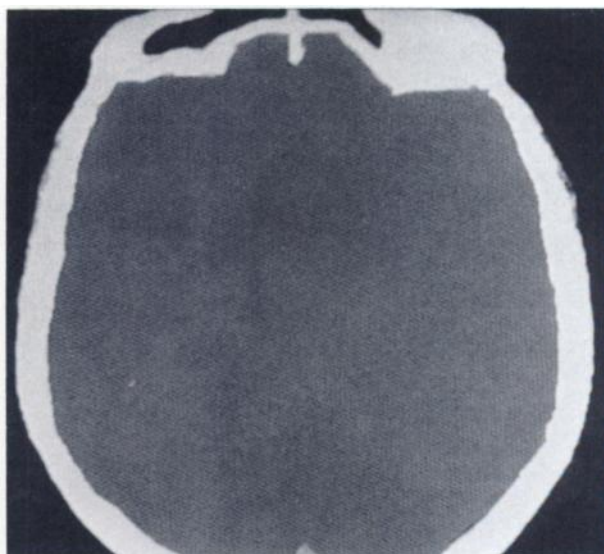
Corrected metabolic rate

= [Uncorrected metabolic rate/relative brain volume (%)]

× 100.

This correction increases the calculated metabolic rates, with the extent of increase dependent upon the degree of atrophy.

All reported XCT atrophy measurements were performed by an observer blinded to the clinical status of the subjects. Since the "volumetric" metabolic and anatomic (atrophy) calculations described above are derived from planar image data, these measurements are in a sense observer-biased esti-

FIGURE 2
Intracranial cavity highlighted (dark gray) via data tablet interface.

mates which could be subjectively influenced by partial volume effects. Although this criticism can only be fully addressed by true volumetric scanning, the reliability of our method is supported by interobserver (ten data pairs) and intraobserver (three data pairs) correlation coefficients (for the relative brain volume measurements) of 0.94 and 0.99, respectively.

RESULTS

Values for the relative ventricular, sulcal, and brain (intracranial cavity minus CSF spaces) volumes as determined from XCT scans are presented in Table 2 and Figure 5. There was significant ventricular and sulcal

FIGURE 1
Digitized image from representative XCT scan section as photographed from video monitor.

FIGURE 3
Ventricular cavity highlighted in light gray.

FIGURE 4
Sulcal spaces highlighted in medium gray.

Mean ± 1 S.D., 24 demented subjects (Alzheimer's disease) (●) and 17 controls (○).

FIGURE 5
Relative degree of ventricular and sulcal atrophy in elderly controls and Alzheimer's (DAT) patients. (%V = percent of intracranial "whole-brain" volume occupied by ventricular CSF. %S = percent of "whole-brain" volume occupied by sulcal CSF. P-values calculated using Student's t-test.)

enlargement in the DAT patients compared to elderly controls (p < 0.001, Student's t-test). The "brain volume" (relative amount of imaged parenchyma) was significantly lower in the dementia group (p < 0.0005) indicating a greater degree of cerebral atrophy in demented patients compared with controls of similar age.

When the whole-brain glucose metabolic rates are corrected for atrophy, there is a significantly greater increase in the dementia cohort compared to elderly controls (p < 0.0005, Table 3). This is an expected consequence of the fact that there is significantly greater atrophy in the demented patients.

In the five DAT patients who had both NMR and XCT scans, we were able to directly compare estimates of atrophy by the two imaging techniques (Fig. 6). Mean ventricular volumes were similar as determined by NMR and XCT, whereas sulcal volumes were significantly larger on the NMR scans (p < 0.02).

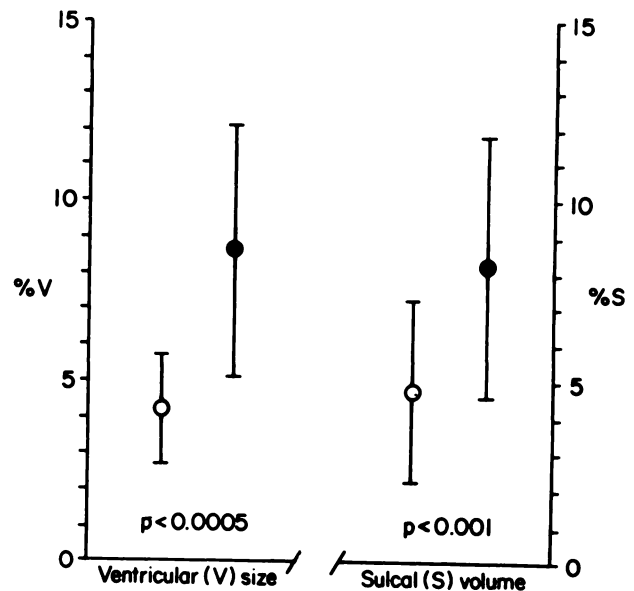## DISCUSSION

Loss of brain mass has long been recognized by neuropathologists as a feature of both dementia and the normal aging process (19). Such observations attracted attempts to measure brain size antemortem, with the hope of increasing pathophysiologic insights into dementia and aging, while improving diagnostic discrimination. Initial reports from the XCT literature were inconclusive, due to convexity artifacts, arbitrary measurement techniques, and relatively inferior scanner res-

TABLE 2
Degree of Cerebral Atrophy*

Diagnosis	Ventricle	Sulci	V + S	Brain
Elderly controls	4.3 (1.5)	4.7 (2.4)	9.0 (3.2)	91.0 (3.2)
Alzheimer's disease (DAT)	8.6 (3.5)‡	8.3 (3.7)†	16.9 (6.1)‡	83.1 (6.1)‡

* Structure volumes expressed as % of intracranial volume. V + S = ventricle + sulci (total atrophy). Brain = relative amount of brain parenchyma imaged by XCT (100 − (V + S)). Values represent means for group with s.d. in parentheses. P-values from Student's t-test comparisons between DAT patients and controls.
 † p < 0.001.
 ‡ p < 0.0005.

TABLE 3
Effect of Atrophy Correction*

Diagnosis	CMRglc_U	CMRglc_C	% Increase CMRglc with atrophy correction
Elderly controls	5.50 (0.9)	6.00 (1.1)	9.0 (3.2)
Alzheimer's disease (DAT)	4.50 (1.2)	5.26 (1.5)	16.9 (6.1)†
% difference (DAT vs. controls)	−18%	−12%	7.9%

* Change in global ("whole-brain") cerebral glucose metabolic rate (CMRglc) after correction for cerebral atrophy. CMRglc expressed as mg/100 g brain/min. CMRglc_U = uncorrected CMRglc. CMRglc_C = CMRglc corrected for atrophy. Values expressed as means with s.d. in parentheses. P-values from Student's t-test comparison of DAT patients with controls.
 † p < 0.001.
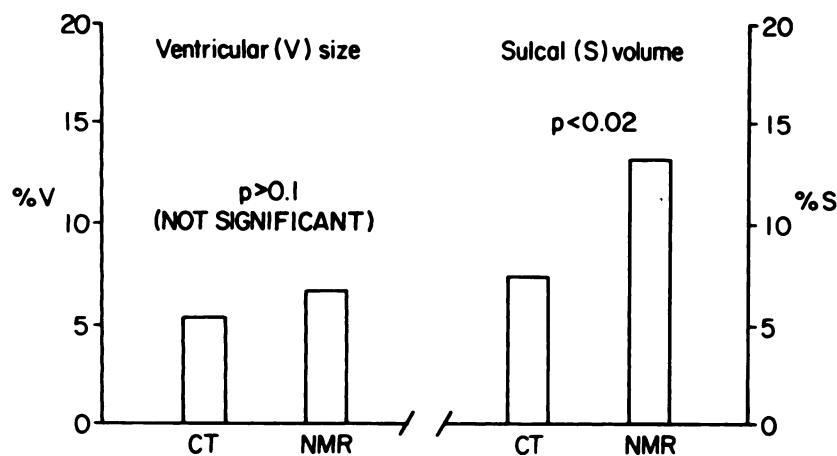
FIGURE 6

Comparison of volumetric atrophy estimates from XCT and proton-NMR transaxial scans (n = 5). See Figure 5 legend (%V, %S). (P-values represent Student's t-test comparisons between Proton-NMR and XCT measurements.)

olution (20-22). These data have been improved upon with the advent of better resolution XCT scanners, along with sophisticated computer programs for image analysis. Gado et al., using a method for estimating relative ventricular and sulcal volumes, noted a highly significant separation of controls from mildly demented patients on the basis of XCT scan atrophic changes (6). Arai et al. from their volumetric XCT atrophy study (7), hypothesized that cortical (sulcal) atrophy was detectable in early (mild) Alzheimer's disease, and that ventricular dilatation was a later (secondary?) occurrence. If their hypothesis is correct, then an imaging modality which more accurately demonstrates sulcal enlargement (proton-NMR?) would in theory prove superior to XCT in diagnosing early dementia. As intuitively expected, additional data from our group (23) indicate that the severity of the cognitive impairment in DAT correlates strongly with the degree of atrophy, thus leading to greater atrophy effects upon metabolic calculations in the more severely demented patients.

In 1956, Kety summarized the results of global cerebral blood flow (CBF) metabolism studies using the Kety-Schmidt technique (1), and correlated these data with estimates of neuronal density changes in aging. His findings indicated a high positive correlation among all three variables; flow, metabolism, and cortical neuronal density decreasing with advancing age (24). Lassen has suggested that increases in the contribution of extracerebral intracranial tissues, including CSF, to mixed jugular blood, could artifactually lower flow and metabolism as measured by the Kety-Schmidt technique (25). Any such error due to cerebral atrophy would be quite small, however, given the extremely slow partitioning of the inert gases into CSF. Atrophy would therefore be expected to exert little direct effect on CBF determined by using any inert gas-diffusible tracer method, including the radioactive isotope clearance techniques for measuring regional CBF developed during the 1960s (3,26).

PET scanning offers definite advantages over isotope clearance techniques by providing three-dimensional tomographic physiological data. A number of centers using PET have reported decreases in global CBF, CMRglc, and oxygen metabolism in patients with dementia (27-31). Based on regional PET data, hypometabolism in Alzheimer's patients appears to be particularly prominent in temporoparietal regions (29,32-34). The PET scanners used in these studies all have an actual in-plane resolution of 1.5-2.0 cm. This relatively poor spatial resolution, in addition to intrinsically low white matter metabolism, leads to an inability to distinguish ventricles and sulci on PET images. Even newer scanners with actual 5-10 mm resolution in-plane (FWHM) do not resolve these structures with the clarity of XCT or proton-NMR (<1 mm resolution). As a result, values for regional and global flow or metabolism, expressed per unit mass of brain tissue, are likely to have been artifactually underestimated due to the inclusion of metabolically inert CSF. Our data reported here indicate that such an error in dementia-elderly control comparisons is on the order of 8% for global GMRglc measurements. Whether reported local metabolic alterations in aging and dementia can in part be explained by focal atrophy requires more complex volumetric XCT or NMR analyses on a regional basis. Preliminary data from our group (35) suggest that significant focal atrophic changes in the parietal lobes of DAT patients may contribute substantially to regional metabolic decrements seen in these areas.

Our finding of greater cortical atrophy on proton-NMR images as compared to XCT scans deserves comment. The limitations of XCT in imaging surfaces next to bone, due to beam hardening artifact and volume averaging, are well known. These problems would lead to probable underestimation of sulcal volumes determined by XCT, as suggested by the preliminary data reported in Figure 6. Proton-NMR scans are not hampered by such artifacts, and in fact cortical bone contributes little or no signal to proton-NMR images (36).

T_2-weighted scans, obtained with spin echo paradigms from late echo images, provide high positive contrast at the CSF-cortex interface (36). We therefore feel that volumetric analyses of such T_2-weighted scans will provide even better measures of cortical atrophy than the T_1-weighted scans used in our analysis here. Such scans should provide the most reliable and accurate anatomic basis for regional atrophy correction in PET studies.

We have not yet directly investigated the effect of atrophy in PET comparisons of young and aged healthy normals. If the age-related progression of atrophy noted with volumetric XCT analyses by others (5,37) is generalized, then PET studies which show no metabolic changes with aging may in fact be demonstrating increased metabolism in the residual brain parenchyma. Inefficient oxidative metabolism, or a compensatory increased utilization of glucose (aerobic or anaerobic) in the residual cerebral tissue could conceivably explain such findings. It may be, however, that in the limited PET series reported to date cerebral atrophy did not play a significant role. In any case our data emphasize the importance of correlative anatomic imaging in PET studies of aging and dementia.

ACKNOWLEDGMENTS

REFERENCES

1. Kety SS, Schmidt CF. The nitrous oxide method for the quantitative determination of cerebral blood flow in man: theory, procedure, and normal values. *J Clin Invest* 1948; 27:476-483.
2. Freyhan FA, Woodford RB, Kety SS. Cerebral blood flow and metabolism in psychoses of senility. *J Nerv Ment Dis* 1951; 113:449-456.
3. Lassen NA, Ingvar DH. Regional cerebral blood flow measurement in man. *Arch Neurol* 1963; 9:615-622.
4. Obrist WD, Thompson HK Jr, Wang HS, et al. Regional cerebral blood flow estimated by ^{133}xenon inhalation. *Stroke* 1975; 6:245-256.
5. Yamaura H, Ito M, Kubota K, et al. Brain atrophy during aging: A quantitative study with computed tomography. *J Gerontology* 1980; 35:492-498.
6. Gado M, Hughes CP, Danziger W, et al. Volumetric measurements of the cerebrospinal fluid spaces in demented subjects and controls. *Radiology* 1982; 144:535-538.
7. Arai H, Kobayashi K, Nagao Y, et al. A computed tomography study of Alzheimer's disease. *J Neurol* 1983; 299:69-77.
8. George AE, De Leon MJ, Rosenbloom S, et al. Ventricular volume and cognitive deficit: A computed tomographic study. *Radiology* 1983; 149:493-498.
9. Diagnostic & Statistical Manual III. American Psychiatric Association, 1980.
10. McKhann G, Drachman D, Folstein M, et al. Clinical diagnosis of Alzheimer's disease. *Neurology* 1984; 34:939-944.
11. Rosen WG, Terry RD, Fuld PA, et al. Pathological verification of ischemic score in differentiation of dementias. *Ann Neurol* 1980; 7:486-488.
12. Folstein M, Folstein S, McHugh PR. Mini-Mental State: a practical method for grading the cognitive state of patients for the clinician. *J Psychiatr Res* 1975; 12:189-198.
13. Reivich M, Kuhl D, Wolf A, et al. The [^{18}F]fluorodeoxyglucose method for the measurement of local cerebral glucose utilization in man. *Circ Res* 1979; 44:127-137.
14. Kushner M, Alavi A, Reivich M, et al. Contralateral cerebellar hypometabolism following cerebral insult: A positron emission tomographic study. *Ann Neurol* 1984; 15:425-434.
15. Ter-Pogossian MM, Mullani NA, Hood JT. Design considerations for a positron emission tomograph (PETT V) for imaging of the brain. *J Comput Assist Tomogr* 1978; 2:539-544.
16. Sokoloff L, Reivich M, Kennedy C, et al. The (^{14}C)-deoxyglucose method for the measurement of local cerebral glucose utilization: theory, procedure, and normal values in the conscious and anesthetized albino rat. *J Neurochem* 1977; 28:897-916.
17. Reivich M, Alavi A, Wolf A, et al. Glucose metabolic rate kinetic model parameter determination in humans: the lumped constants and rate constants for [^{18}F]fluorodeoxyglucose and [^{11}C]deoxyglucose. *J Cereb Blood Flow Metab* 1985; 5:179-192.
18. Edelstein WA, Bottomley PA, Hart HR, et al. Signal, noise and contrast in nuclear magnetic resonance (NMR) imaging. *J Comput Assist Tomogr* 1983; 7:391-401.
19. Tomlinson BE: The structural and quantitative aspects of the dementias. In: Roberts PJ, ed. Biochemistry of Dementia. Chichester: John Wiley & Sons, 1980: 15-52.
20. Jacoby RJ, Levy R, Dawson JM. Computed tomography in the elderly: I. The normal population. *Br J Psychiatr* 1980; 136:249-255.
21. Jacoby RJ, Levy R. Computed tomography in the elderly: 2. Senile dementia: Diagnosis and functional impairment. *Br J Psychiatr* 1976; 39:909-915.
22. Roberts MA, Caird FI, Grossart KW, et al. Computerized tomography in the diagnosis of cerebral atrophy. *J Neurol Neurosurg Psychiatr* 1976; 39:909-915.
23. Chawluk J, Alavi A, Hurtig H, et al. Cerebral atrophy is highly correlated with the severity of Alzheimer's dementia: A volumetric computed tomographic study. *Neurology* 1986; 36(suppl 1):264.
24. Kety SS. Human cerebral blood flow and oxygen consumption as related to aging. *J Chronic Dis* 1956; 3:478-486.
25. Lassen NA. Cerebral blood flow and oxygen consumption in man. *Physiol Rev* 1959; 39:183-238.
26. Mallett BL, Veall N. Measurement of regional cerebral clearance rates in man using xenon-133 inhalation and extracranial recording. *Clin Sci* 1965; 29:179-191.
27. Alavi A, Ferris S, Wolf A, et al. Determination of cerebral metabolism in senile dementia using F-18-deoxyglucose and positron emission tomography. *J Nucl Med* 1980; 21:21.
28. Ferris SH, de Leon MJ, Wolf AP, et al. Positron

emission tomography in the study of aging and senile dementia. *Neurobiol Aging* 1980; 1:127–131.

29. Frackowiak RSJ, Pozzilli C, Legg NJ, et al. Regional cerebral oxygen supply and utilization in dementia—a clinical and physiological study with oxygen-15 and positron tomography. *Brain* 1981; 104:753–778.

30. Farkas T, Ferris SH, Wolf AP, et al. 18F-2-deoxy-2-fluro-D-glucose as a tracer in the positron emission tomographic study of senile dementia. *Am J Psychiatr* 1982; 139:352–353.

31. Kuhl DE, Metter EJ Riege WH, et al. Local cerebral glucose utilization in elderly patients with depression, multiple infarct dementia, and Alzheimer's disease. *J Cerebr Blood Flow Metab* 1983; 3 (suppl 1):S494–495.

32. Duara R, Grady C, Haxby J, et al. Positron emission tomography in Alzheimer's disease. *Neurology* 1986; 36:879–887.

33. Friedland RP, Budinger TF, Ganz E, et al. Regional cerebral metabolic alterations in dementia of the Alz-heimer type: positron emission tomography with [^{18}F] fluorodeoxyglucose. *J Comp Assist Tomogr* 1983; 7:590–598.

34. Benson DF, Kuhl DE, Hawkins RA, et al. The fluorodeoxyglucose ^{18}F scan in Alzheimer's disease and multi-infarct dementia. *Arch Neurol* 1983; 40:711–714.

35. Chawluk J, Alavi A, Hurtig H, et al. Positron emission tomography (PET) in brain aging and dementia: the effect of focal atrophy on regional metabolic calculations. *J Nucl Med* 1986; 27:945.

36. Buonanno FS, Pykett IL, Brady TJ, et al. Clinical applications of nuclear magnetic resonance (NMR). *Dis Month* 1983; 29(8):1–81.

37. Ito M, Hatazawa J, Yamaura H, et al. Age-related brain atrophy and mental deterioration—a study with computed tomography. *Br J Radiol* 1981; 54:384–390.